



Computation of steady-state operating conditions of a DFIG-based wind energy conversion system considering losses

D. R. Karthik¹ · Narayan S. Manjarekar¹ · Shashidhara Mecha Kotian²

Received: 23 September 2022 / Accepted: 26 January 2023 / Published online: 23 February 2023
© The Author(s), under exclusive licence to Springer-Verlag GmbH Germany, part of Springer Nature 2023

Abstract

In this paper, steady-state operating conditions of a doubly fed induction generator (DFIG) are computed considering losses of grid-side (GS) filter. Two different cases are studied for steady-state initialization of the DFIG-based wind turbine systems (WTS). In the first case, active power (P) and reactive power (Q) at DFIG terminals are assumed to be known. In the other case wind speed (V_w), Q is assumed to be known. Apart from considering losses of the DFIG and GS filter, both the cases also consider the non-unity power factor operation of the grid side converter (GSC). For the first case, steady-state operating conditions are calculated by iterative method as well as by non-iterative method. For the second case, iterative method is used to calculate steady-state operating conditions. Calculation of steady-state values of other subsystems of DFIG-based WTS like drive train, controller and network is also shown. The initial values calculated are validated and compared by performing modal analysis and time-domain simulations.

Keywords Doubly fed induction generator · Steady-state operating points · Non-iterative method · Iterative method · Grid-side filter · Modal analysis · Time-domain simulations

1 Introduction

The integration of type-3 or DFIG-based WTS is high in present-day power systems. High efficiency, less stress on mechanical components, and the potential of reactive power delivery to grid make DFIG a viable alternative to include in the power system network. On the other hand, the penetration of these converter interfaced machines (CIM) into the power system needs to be thoroughly investigated in stability point-of-view. Negative consequences if any, arising from these CIM needs to be addressed by appropriate control mechanism. Eigenvalue analysis and time-domain simulations are

utilized to observe the change in dynamics of overall system, caused by these CIM. Before studying the dynamics of DFIG-connected power system, steady-state initial values must be calculated. Accurate steady-state values aid in properly initializing dynamic investigations before the occurrence of the actual fault, and also to avoid numerical instability [1, 2].

Steady-state initialization of a DFIG-based WTS can be carried out by using basic circuit laws [3], by iterative methods [4–9], or by using non-iterative methods [10–13]. The methods available for steady-state initialization of a DFIG-based WTS are broadly classified as electromagnetic transient programme (EMTP)-based approach and load flow-based approach. EMTP-based approaches use phasor-based technique [14], which deals with non-linear and time-variant systems for small, linear with lumped component networks. However, for a large system, the EMTP-type approach becomes inefficient due to high computational burden and solution may not converge to desirable operating points. On the other hand, load flow programmes are suitable for large systems using minimal mathematical effort. Load flow approach is not suitable for time-variant systems. However, is suitable for both balanced and unbalanced systems. Steady-state model of the DFIG reflects the operation of the DFIG

✉ D. R. Karthik
p20170426@goa.bits-pilani.ac.in

Narayan S. Manjarekar
narayan@goa.bits-pilani.ac.in

Shashidhara Mecha Kotian
shashikotian@nitk.edu.in

¹ Department of Electrical and Electronics Engineering, BITS Pilani K. K. Birla Goa Campus, Zuari Nagar, Goa 403726, India

² Department of EEE, National Institute of Technology Karnataka, Surathkal, NH 66, Srinivasnagar, Mangalore, Karnataka 575025, India

during non-transient state. It should properly represent the power flows and losses. The final steady-state values derived from the steady-state model considered should initialize the DFIG without any initial oscillations.

Various models representing the steady-state behaviour of a DFIG are available in the literature. The steady-state model is represented as two-port circuit either in T model [15] or π model [16]. Numerous steady-state equivalent circuits of DFIG like PQ model [17], RX model [18] are available in the literature. The equivalent circuit of the DFIG should also consider the GS filter circuit so that filter losses also be taken into account. Calculation of initial values begins with the assumption that DFIG is operating at known active and reactive power at its terminals or wind power and reactive power assumed to be known parameters.

In [10] describes how to initialize various types of wind turbines, including type-3-based wind turbines, but the generator losses are ignored and the flow of reactive power flow through the GSC is assumed to be zero. Concept of torque balancing is used by the author of [11] to initialize full and lower-order models of DFIG. Calculation of initial values including unknown parameters within initialization procedure is shown in [4], but this method is complicated and tedious. Reference [5] uses as PV, PQ and $V_w - Q$ method and uses the Newton–Raphson (NR) algorithm to calculate initial values without using d-q terms. The author of [13] considered the rotor of DFIG as a current source and calculates the initial values by a non-repetitive method. A direct method to calculate the initial values of DFIG-based WTS is shown in [12].

In most of these works, losses of GS filter are ignored. This paper considers the GS filter loss in the initialization procedure and also considers non-zero reactive power flow through GSC ($Q_{gsc} \neq 0$) in the two initialization methods employed. A procedure to calculate steady-state values of other subsystems of DFIG-WTS is also given. Finally, steady-state values are evaluated by eigenvalue analysis and time-domain simulations to examine effectiveness of the initialization methods employed.

The objectives of this paper are: (a) To perform steady-state initialization of a DFIG considering losses of machine and grid-side filter. (b) Utilizing both iterative and non-iterative methods for steady-state initialization, and to compare the performance of both the methods. (c). To calculate steady-state initial values of other subsystems of WTS like turbine, controller, network and DC link capacitor. (d) To validate the steady-state values obtained from eigenvalue analysis and time-domain simulations.

The organization of paper is as follows: Sect. II discusses the steady-state modelling and initialization of a DFIG-based WTS for two different cases. In Sect. III, dynamic modelling of a DFIG-based WTS is shown. In Sect. IV, case studies are conducted on a DFIG connected to a infinite bus system

to validate the steady-state values obtained in Sect. II by performing modal analysis and time-domain simulations. In Sect. V, concluding remarks of the present work are given.

2 Steady-state modelling of DFIG

2.1 DFIG-based WTS

In Fig. 1, the block diagram representation of the DFIG-based WTS is shown where the turbine is coupled to the generator through a gear-box. Stator of the DFIG is directly connected to grid, and the rotor is interfaced to grid via a partial rated back-to-back converter. The converters are controlled by their respective controllers which help in smooth operation of the system [19]. RSC controller coordinates with the wind turbine control to extract maximum power by tracking optimum power points and also help in limiting the mechanical power generated by the turbine system by controlling its pitch angle. The generated mechanical power of wind turbine can be expressed as [20]

$$P_m = \frac{1}{2} \rho A C_p V_w^3 \quad (1)$$

where ρ = density of air in kg/m^3 , A = area of turbine blades in m^2 , C_p = performance co-efficient, V_w = wind velocity in m/s , S_b = MVA base, $\omega_{r,t}$ = rotor speed of the turbine. Details of C_p and other turbine parameters are referred from [10] and are provided in appendix A.

$$P_m = k_{\text{opt}}(1 - s)^3 \quad (2)$$

Apart from controlling the electromagnetic torque, RSC controller has to control reactive power supplied to the grid through stator, by supplying necessary rotor currents into the generator. The objective of a GSC controller is to maintain a constant terminal voltage and to keep voltage across DC-link capacitor constant by which rotor active power will be equal to GSC active power ($P_r = P_{gsc}$).

2.2 Modelling of DFIG in steady-state

The steady-state model of a DFIG including the GS filter is shown in Fig. 2.

$$\vec{V}_s = (R_s + jX_s)\vec{I}_s + jX_m(\vec{I}_r + \vec{I}_s) \quad (3a)$$

$$\frac{\vec{V}_r}{s} = \left(\frac{R_r}{s} + jX_r \right) \vec{I}_r + jX_m(\vec{I}_r + \vec{I}_s) \quad (3b)$$

where $\vec{V}_s = v_s \angle \delta_s$ and $\vec{V}_r = v_r \angle \delta_r$ are stator and rotor voltage phasors, respectively. $\vec{I}_s = i_s \angle \gamma_s$, $\vec{I}_r = i_r \angle \gamma_r$,

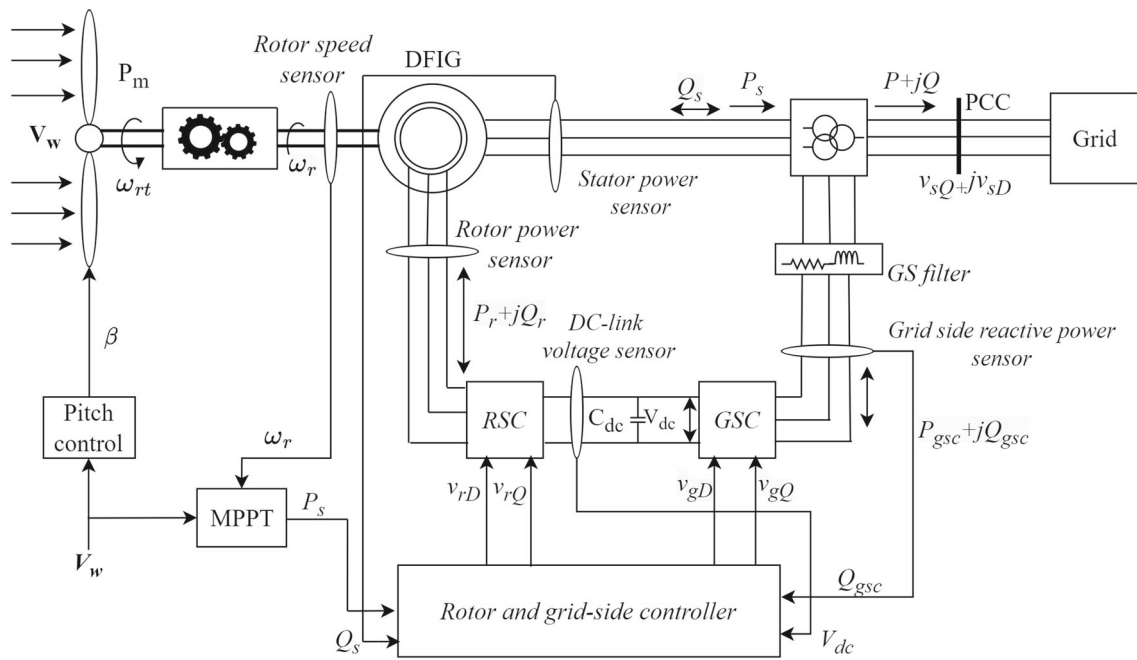


Fig. 1 Schematic of DFIG

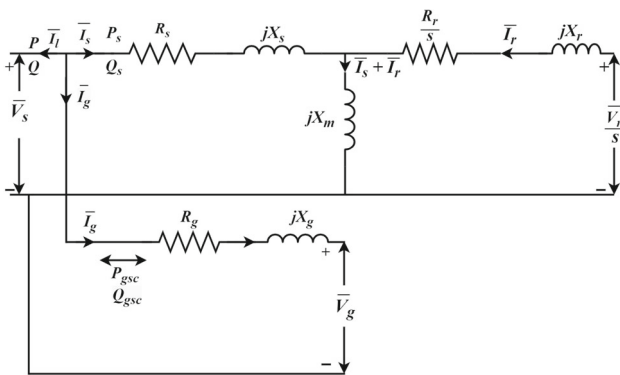


Fig. 2 Steady-state model of DFIG including filter

$\vec{I}_g = i_g \angle \gamma_g$ are stator, rotor and grid-side current phasors, respectively. The total current is given as

$$-\vec{I}_l = \vec{I}_s + \vec{I}_g \tag{4}$$

The reactive power flow through GSC is

$$Q_{gsc} = V_s I_g \sin(\delta_s - \gamma_g) \tag{5}$$

Here, the line current I_l is assumed to be negative, due to motoring convention followed.

The losses of the GS filter are given as

$$I_g^2 R_g = P_r - P_{gsc} \tag{6}$$

2.3 Steady-state initialization in PQ method

The set of non-linear equations of PQ method can be solved by both iterative and non-iterative methods. NR procedure is used to calculate initial values iteratively. To solve these equations by non-iterative method, the set of non-linear DFIG equations are rearranged into solvable quadratic equation. Both iterative and non-iterative methods are discussed in following subsections.

2.3.1 Steady-state initialization using iterative method

Equations related to NR method for initialization are shown as follows.

Iterative function at k^{th} iteration for NR method is given as

$$\underline{x}_{k+1} = \underline{x}_k - [J]_k^{-1} F(\underline{x}_k) \tag{7}$$

where $F(\underline{x}) = [f_1, f_2, \dots, f_8]^T$, is a set of n equations corresponding to (8a)–(11) which are functions of unknown variable, \underline{x} and $[J]_k$ is the $(n \times n)$ Jacobian matrix which contains partial derivatives of the functions $F(\underline{x})$ with respect to the variables in \underline{x} .

The unknown variables are $\underline{x} = [i_{sQ}, i_{sD}, i_{rQ}, i_{rD}, v_{rQ}, v_{rD}, i_{gQ}, i_{gD}]^T$

The initial values of vector \underline{x} are taken as

$$\underline{x}_0 = [0.5, 0.5, 0.5, 0.5, 0.5, 0.5, 0.5, 0.5]^T$$

The functions $f_1 - f_8$ correspond to Eqs. (8a)–(11),

$$f_1 = v_{sQ} - R_s i_{sQ} + (X_s + X_m) i_{sD} + X_m i_{rD} \quad (8a)$$

$$f_2 = v_{sD} - R_s i_{sD} - (X_s + X_m) i_{sQ} - X_m i_{rQ} \quad (8b)$$

$$f_3 = v_{rQ} - R_r i_{rQ} + s(X_r + X_m) i_{rD} + s X_m i_{sD} \quad (8c)$$

$$f_4 = v_{rD} - R_r i_{rD} - s(X_r + X_m) i_{rQ} - s X_m i_{sQ} \quad (8d)$$

The total current supplied by DFIG is equal to sum of stator current and current supplied by GSC

$$f_5 = i_{lQ} + i_{sQ} + i_{gQ} \quad (9a)$$

$$f_6 = i_{lD} + i_{sD} + i_{gD} \quad (9b)$$

In this work, the reactive power supplied by GSC is assumed to be non-zero

$$f_7 = Q_{gsc} - v_{gD} i_{gQ} + v_{gQ} i_{gD} \quad (10)$$

The power loss occurring at the grid-side filter is the difference between rotor active power and grid-side active power, i.e. $P_r - P_{gsc}$

$$f_8 = v_{rQ} i_{rQ} + v_{rD} i_{rD} - v_{sQ} i_{gQ} - v_{sD} i_{gD} - i_{gD}^2 R_g - i_{gQ}^2 R_g \quad (11)$$

The values of unknown vector \underline{x} are obtained by solving (7), with initial values assumed in \underline{x}_0 . Figure 3 shows the flow chart defining iterative-based PQ initialization method.

2.3.2 Initialization using non-iterative method

The initial values are calculated non-iteratively using substitution method. The DFIG bus is treated as PQ bus where active and reactive power at DFIG terminals is known. From P and Q , stator voltage, i.e. (v_{sQ} and v_{sD}) is calculated by applying fixed point iterative method [9]. The active power (P) is assumed to be equal to input mechanical power (P_m). The slip s corresponding to (P_m) is calculated from (2). Values of Q and Q_{gsc} are assumed to be known. Other variables, i.e. stator current (i_{sQ} , i_{sD}), rotor voltage (v_{rQ} , v_{rD}), rotor current (i_{rQ} , i_{rD}), and GSC currents (i_{gQ} , i_{gD}), are calculated by procedure shown as follows:

Referring equation (10), the i_{gQ} is given as

$$i_{gQ} = \frac{Q_{gsc}}{v_{sD}} + \frac{v_{sQ}}{v_{sD}} i_{gD} \quad (12)$$

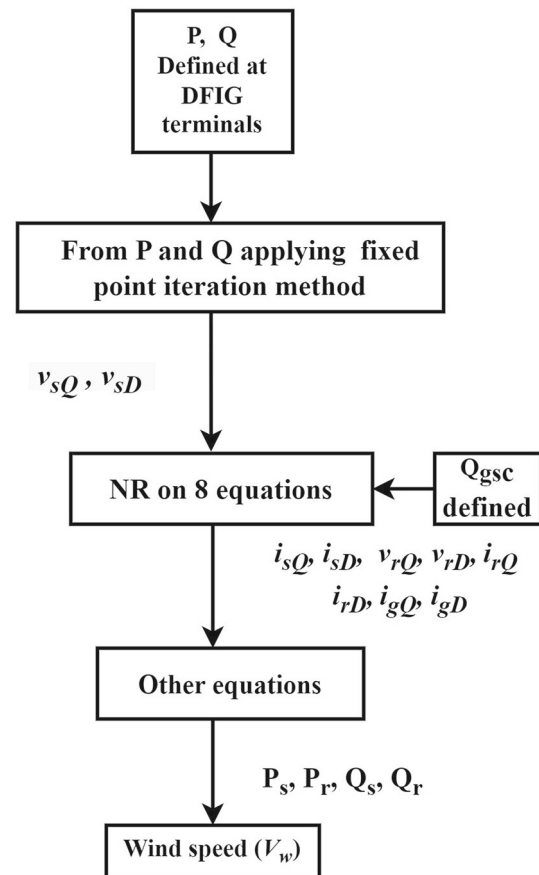


Fig. 3 Flowchart depicting PQ initialization procedure

Substituting (12) in (9a), i_{sQ} is written as

$$i_{sQ} = -i_{lQ} - \frac{Q_{gsc}}{v_{sD}} - \frac{v_{sQ}}{v_{sD}} i_{gD} \quad (13)$$

From (9b) i_{sD} is written as

$$i_{sD} = -i_{lD} - i_{gD} \quad (14)$$

Substituting (13) and (14) in (8a), the i_{rD} is written as

$$i_{rD} = \left(\frac{-R_s v_{sQ}}{X_m v_{sD}} + \frac{X_s + X_m}{X_m} \right) i_{gD} + \left(-\frac{R_s}{X_m} i_{lQ} - \frac{R_s Q_{gsc}}{X_m v_{sD}} + \frac{X_s + X_m}{X_m} i_{lD} - \frac{v_{sQ}}{X_m} \right) \quad (15a)$$

$$i_{rD} = a_1 i_{gD} + b_1 \quad (15b)$$

Substituting (13) and (14) in (8b), the i_{rQ} is written as

$$i_{rQ} = \left(\frac{R_s}{X_m} + \frac{X_s + X_m}{X_m} \frac{v_{sQ}}{v_{sD}} \right) i_{gD} + \left(\frac{R_s}{X_m} i_{lD} + \frac{X_m + X_m}{X_m} \frac{Q_{gsc}}{v_{sD}} \right) + \left(\frac{X_s + X_m}{X_m} i_{lQ} + \frac{v_{sD}}{X_m} \right) \tag{16a}$$

$$i_{rQ} = a_2 i_{gD} + b_2 \tag{16b}$$

Substituting (14), (15b) and (16b) in (8c)

$$v_{rQ} = (R_r a_2 - s(X_r + X_m) a_1 + s X_m) i_{gD} + (R_r b_2 - s(X_r + X_m) b_1 + s X_m i_{lD}) \tag{17a}$$

$$v_{rQ} = a_3 i_{gD} + b_3 \tag{17b}$$

Substituting (14), (15b) and (16b) in (8d)

$$v_{rD} = \left(R_r a_1 + s(X_r + X_m) a_2 - s X_m \frac{v_{sQ}}{v_{sD}} \right) i_{gD} + \left(R_r b_1 + s(X_r + X_m) b_2 - s X_m i_{lQ} - s X_m \frac{Q_{gsc}}{v_{sD}} \right) \tag{18a}$$

$$v_{rD} = a_4 i_{gD} + b_4 \tag{18b}$$

Substituting (12)–(21d) in (11) we get i_{gD} as

$$a_5 i_{gD}^2 + b_5 i_{gD} + c_5 = 0 \tag{19}$$

where

$$a_5 = \frac{v_{sQ}^2}{v_{sD}^2} R_g - a_3 a_2 - a_4 a_1 + R_g$$

$$b_5 = v_{sD} + 2 \frac{v_{sQ}}{v_{sD}^2} Q_{gsc} R_g + \frac{v_{sQ}^2}{v_{sD}^2} - a_3 b_2 - a_2 b_3 - a_4 b_1 - a_1 b_4$$

$$c_5 = \frac{Q_{gsc}^2}{v_{sD}^2} R_g - b_2 b_3 - b_1 b_4 + \frac{v_{sQ}}{v_{sD}} Q_{gsc}$$

The quadratic solution of i_{gD} is obtained by solving (19)

$$i_{gD} = \frac{-b_5 \pm \sqrt{b_5^2 - 4a_5c_5}}{2a_5} \tag{20}$$

Solving Eq. (20) results in two values of i_{gD} ; however, only one value of i_{gD} results in stable operating point. By substituting the stable i_{gD} in (12)–(18b), the steady-state parameters of the DFIG are obtained.

In Table 1, comparison of the initial values obtained from both iterative and non-iterative method for $P = 0.68$, $Q = 0.2$, $Q_{gsc} = 0.1$ is made, all values are in per unit (pu). It is seen that steady-state values are not exactly equal but are close. Steady-state values computed from non-iterative approach do not have rounding-off errors as for

Table 1 Comparison of steady-state values calculated from iterative and non-iterative method for PQ case

$P = 0.68, Q = 0.2, Q_{gsc} = 0.1$		
Variable	Iterative	Non-iterative
i_{sD}	0.2836	0.2834
i_{sQ}	-0.6799	0.6711
v_{rD}	-0.00419	-0.0042
v_{rQ}	-0.00468	-0.0047
i_{rD}	-0.5459	-0.5456
i_{rQ}	0.7008	0.6918
i_{gD}	-0.0993	-0.0992
i_{gQ}	-0.00096	-0.0022

iterative methods. Also, an accurate initial guess is needed for iterative methods to prevent system from non-convergence, while in non-iterative method, no initial guess is needed. It can be concluded that initial values calculated from non-iterative methods are accurate and have faster convergence. The advantages of non-iterative methods make it preferable for computing steady initial operating points of DFIG.

2.4 Steady-state initialization in V_w -Q method

Another method of solving initialization problem of DFIG is to consider wind speed (V_w) to be known. Mechanical power developed by wind turbine depends on the speed of the wind. As wind speed is variable in nature, assuming wind speed as constant value makes the initialization method more accurate. The equations considered for $V_w - Q$ method can be solved only by iterative methods and cannot be rearranged such that these equations can be solved linearly. From the wind speed mechanical power developed is calculated. In this method apart from wind speed Q and Q_{gsc} are assumed to be known parameters.

After calculating mechanical power developed from wind speed, corresponding slip is calculated from Eq. (2). Unknown parameters of DFIG, i.e. stator voltage and current ($v_{sQ}, v_{sD}, i_{sQ}, i_{sD}$), rotor voltage and current ($v_{rQ}, v_{rD}, i_{rQ}, i_{rD}$) and GSC currents and voltages ($i_{gQ}, i_{gD}, v_{gQ}, v_{gD}$), are calculated by applying NR-based iterative method in Eqs. (21a)–(21l).

Figure 4 depicts the flow chart depicting initialization procedure for $V_w - Q$ case.

$$f_1 = v_{sQ} - R_s i_{sQ} + (X_s + X_m) i_{sD} + X_m i_{rD} \tag{21a}$$

$$f_2 = v_{sD} - R_s i_{sD} - (X_s + X_m) i_{sQ} - X_m i_{rQ} \tag{21b}$$

$$f_3 = v_{rQ} - R_r i_{rQ} + s(X_r + X_m) i_{rD} + s X_m i_{sD} \tag{21c}$$

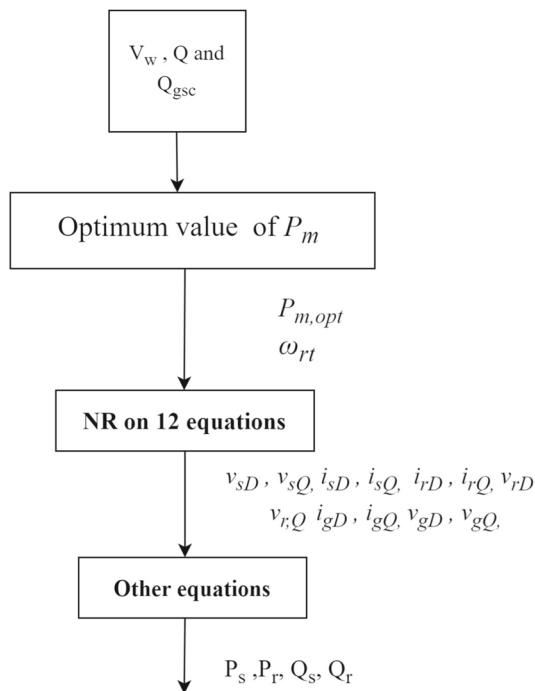


Fig. 4 Flowchart depicting $V_w - Q$ initialization procedure

$$f_4 = v_{rD} - R_r i_{rD} - s(X_r + X_m)i_{rQ} - sX_m i_{sQ} \quad (21d)$$

$$f_5 = Q - v_{sQ}i_{sD} + v_{sD}i_{sQ} - v_{gQ}i_{gD} + v_{gD}i_{gQ} \quad (21e)$$

$$f_6 = P_m - P - (i_{sQ}^2 + i_{sD}^2)R_s - (i_{rQ}^2 + i_{rD}^2)R_r - (i_{gQ}^2 + i_{gD}^2)R_g \quad (21f)$$

$$f_7 = Q_{gsc} - v_{gD}i_{gQ} + v_{gQ}i_{gD} \quad (21g)$$

$$f_8 = v_{sQ} - v_{1Q} - \frac{Pa + Qb}{v_{sQ}^2 + v_{sD}^2} \quad (21h)$$

$$f_9 = v_{sD} - v_{1D} - \frac{Pb - Qa}{v_{sQ}^2 + v_{sD}^2} \quad (21i)$$

$$f_{10} = v_{rQ}i_{rQ} + v_{rD}i_{rD} - v_{gQ}i_{gQ} - v_{gD}i_{gD} \quad (21j)$$

$$f_{11} = v_{sQ} - v_{gQ} - R_g i_{gQ} - L_g i_{gD} \quad (21k)$$

$$f_{12} = v_{sD} - v_{gD} - R_g i_{gD} - L_g i_{gQ} \quad (21l)$$

where

$$P = -((v_{sQ}i_{sQ} + v_{sD}i_{sD}) + (v_{rQ}i_{rQ} + v_{rD}i_{rD}))$$

$$a = (v_{sQ}Z_{1Q} - v_{sD}Z_{1D})$$

$$b = (v_{sQ}Z_{1D} + v_{sD}Z_{1Q})$$

Due to the motoring convention employed in this work, mechanical power developed by wind turbine is assumed as negative, i.e. $-P_m$. NR-based iterative method is used to solve the set of 12 non-linear equations to obtain 12 unknown parameters of the DFIG.

Table 3 lists DFIG steady-state values in pu calculated employing iterative method for case index listed in Table 2. In case A of Table 2, V_w is assumed to be 12.5 m/s, corresponding to supersynchronous speeds and Q , Q_{gsc} are assumed zero. In case B wind speed V_w corresponds to supersynchronous and Q , Q_{gsc} are assumed to be non-zero. Case C corresponds to subsynchronous speed with wind speed 7.5 m/s and Q , Q_{gsc} are made zero. Case D corresponds to subsynchronous speed with Q , Q_{gsc} are assumed to be non-zero.

The reactive power flow from rotor side to grid is given as

$$Q_{gsc} = v_{gD}i_{gQ} - v_{gQ}i_{gD} \quad (22)$$

2.5 Initialization of other models of WTS

After computing the steady-state initial values of the DFIG, initialization of various other models in WTS is carried out using approach followed.

Wind turbine initialization:

Wind turbine initial values are calculated starting with known steady-state value of s obtained from Eq. 2 for a particular operating condition.

$$\omega_r = 1 - s \quad (23a)$$

$$\omega_{rt} = \omega_r \quad (23b)$$

$$\lambda = \frac{\omega_{rt}\omega_{rtmBR}}{V_w} \quad (23c)$$

$$\lambda_i = \frac{(\beta^3\lambda + \lambda + 0.08\beta^4 + 0.08\beta)}{(\beta^3 + 1 - 0.035\lambda - 0.0028\beta)} \quad (23d)$$

$$C_p = c1\left(\frac{c2}{\lambda_i} - c3\beta - c4\right)e^{(-c5/\lambda_i)} \quad (23e)$$

$$T_{Tg} = (D_g\omega_r - T_e) \quad (23f)$$

Network parameters initialization:

$$i_{lQ} = (v_{sQ}/R_L) + i_{sQ} + i_{gQ} \quad (24a)$$

$$i_{lD} = (v_{sD}/R_L) + i_{sD} + i_{gD} \quad (24b)$$

DFIG controller initialization:

$$i_{rQF} = i_{rQ} - K_{pT}(k_{opt}\omega_r^2 + T_e) \quad (25a)$$

Table 2 Index of case studies of $V_w - Q$ method

Case	Mode	$V_w(m/s)$	$Q(pu)$	$Q_{gsc}(pu)$	$P_m(pu)$	Slip
A	$\omega_r > \omega_s$	12.5	0	0	0.938	-0.1185
B	$\omega_r > \omega_s$	12.5	0.2	0.1	0.938	-0.1185
C	$\omega_r < \omega_s$	7.5	0	0	0.2026	0.3289
D	$\omega_r < \omega_s$	7.5	0.2	0.1	0.2026	0.3289

Table 3 Steady-state values of DFIG for V_w -Q case at various operating points

Case index	v_{sQ}	v_{sD}	i_{sQ}	i_{sD}	v_{rQ}	v_{rD}	i_{rQ}	i_{rD}	i_{gQ}	i_{gD}	v_{gQ}	v_{gD}
Case A	1.001	0.0303	-0.8478	-0.0256	-0.1167	-0.0244	0.8753	-0.2280	-0.0965	0.0027	0.9998	0.0281
Case B	1.0073	0.0298	-0.8459	0.0742	-0.1198	-0.0249	0.8731	-0.3318	-0.0928	-0.1016	1.0008	0.0266
Case C	1.0004	0.0065	-0.3053	-0.002	0.3394	0.0203	0.3141	-0.2514	0.1013	0.0008	1.0016	0.0088
Case D	1.0067	0.0061	-0.3051	0.0975	0.3479	0.0195	0.3136	-0.3548	0.1019	-0.0983	1.0102	0.0072

$$v_{rQ1} = v_{rQ} - K_{pq}(i_{rQF} + K_{pT}k_{opt}\omega_r^2 + K_{pT}T_e - i_{rQ}) \tag{25b}$$

$$i_{gDF} = i_{rD} - K_{pQ}(Q_{s,ref} - Q_s) \tag{25c}$$

$$v_{rD1} = v_{rD} - K_{pd}(i_{rDF} + K_{pQ}(Q_{s,ref} - Q_s) - i_{rD}) \tag{25d}$$

$$Q_s = v_{sD}i_{sQ} - v_{sQ}i_{sD} \tag{25e}$$

$$i_{gQF} = i_{gQ} - K_{p4}(v_{dc,ref} - v_{dc}) \tag{25f}$$

$$v_{gQ1} = v_{gQ} - K_{p3}(i_{gQF} + K_{p4}(v_{dc,ref} - v_{dc}) - i_{gQ}) \tag{25g}$$

$$i_{gDF} = i_{gD} - K_{p4}(v_{t,ref} - v_t) \tag{25h}$$

$$v_{gD1} = v_{gD} - K_{p3}(i_{gDF} + K_{p4}(v_{t,ref} - v_t) - i_{gD}) \tag{25i}$$

$$Q_g = v_{sD}i_{gQ} - v_{sQ}i_{gD} \tag{25j}$$

DC-link capacitor initialization:

$$v_{dc0} = v_{dc} \tag{26}$$

Steady-state values of turbine, DFIG controller, network and filter are used for eigenvalue analysis and time-domain simulations.

3 Dynamic modelling of DFIG-based WTS

3.1 Drive train model

The two-mass model is used to represent dynamic model of the drive train. Three equations corresponding to shaft, turbine and generator used are [21].

$$2H_t \frac{d\omega_{rt}}{dt} = T_w - T_{tg} - D_{tg}(\omega_{rt} - \omega_r) - D_t(\omega_{rt}) \tag{27a}$$

$$2H_g \frac{d\omega_r}{dt} = T_{tg} + D_{tg}(\omega_{rt} - \omega_r) - D_g(\omega_r) + T_e \tag{27b}$$

$$\frac{dT_{tg}}{dt} = K_{tg}(\omega_{rt} - \omega_r)\omega_B \tag{27c}$$

3.2 DFIG dynamic modelling

Dynamic equations of full order model of DFIG are expressed as follows [22].

$$\frac{1}{\omega_B} \frac{d\psi_{sQ}}{dt} = v_{sQ} - R_s i_{sQ} + \omega_0 \psi_{sD} \tag{28a}$$

$$\frac{1}{\omega_B} \frac{d\psi_{sD}}{dt} = v_{sD} - R_s i_{sD} - \omega_0 \psi_{sQ} \tag{28b}$$

$$\frac{1}{\omega_B} \frac{d\psi_{rQ}}{dt} = v_{rQ} - R_r i_{rQ} + (\omega_0 - \omega_r) \psi_{rD} \tag{28c}$$

$$\frac{1}{\omega_B} \frac{d\psi_{rD}}{dt} = v_{rD} - R_r i_{rD} - (\omega_0 - \omega_r) \psi_{rQ} \tag{28d}$$

The developed torque by DFIG is given as

$$T_e = \psi_{rD}i_{rQ} - \psi_{rQ}i_{rD} \tag{29}$$

The currents of DFIG are related to stator and rotor flux as follows:

$$\begin{bmatrix} i_{sD} \\ i_{sQ} \\ i_{rD} \\ i_{rQ} \end{bmatrix} = \begin{bmatrix} X_{ss} & 0 & X_m & 0 \\ 0 & X_{ss} & 0 & X_m \\ X_m & 0 & X_{rr} & 0 \\ 0 & X_m & 0 & X_{rr} \end{bmatrix}^{-1} \begin{bmatrix} \psi_{sD} \\ \psi_{sQ} \\ \psi_{rD} \\ \psi_{rQ} \end{bmatrix}$$

where $X_{ss} = X_s + X_m$, $X_{rr} = X_r + X_m$.

3.3 Interface equations of DFIG to network

The equations for interfacing the DFIG to network are expressed in synchronous reference frame as

$$v_{sD} = [i_{lD} - (i_{sD} + i_{gD})]R_L \tag{30a}$$

$$v_{sQ} = [i_{lQ} - (i_{sQ} + i_{gQ})]R_L \tag{30b}$$

A high resistance R_L with value of 100 pu is connected at DFIG terminals to avoid redundant states.

3.4 Grid-side filter dynamic model

The dynamic equations of the GS filter are written as

$$\frac{di_{gQ}}{dt} = -\frac{\omega_B R_g}{L_g} i_{gQ} + \omega_B i_{gD} + \frac{\omega_B}{L_g} v_{gQ} - \frac{\omega_B}{L_g} v_{sQ} \tag{31a}$$

$$\frac{di_{gD}}{dt} = -\frac{\omega_B R_g}{L_g} i_{gD} - \omega_B i_{gQ} + \frac{\omega_B}{L_g} v_{gD} - \frac{\omega_B}{L_g} v_{sD} \tag{31b}$$

3.5 Network model

The dynamic equations of the line connecting DFIG and infinite bus are shown as [23]

$$\frac{di_{lD}}{dt} = \frac{1}{L_{lt}} [e_D - R_l i_{lD} - L_{lt} \omega_B i_{lQ} - v_{sD}] \tag{32a}$$

$$\frac{di_{lQ}}{dt} = \frac{1}{L_{lt}} [e_Q - R_l i_{lQ} + L_{lt} \omega_B i_{lD} - v_{sQ}] \tag{32b}$$

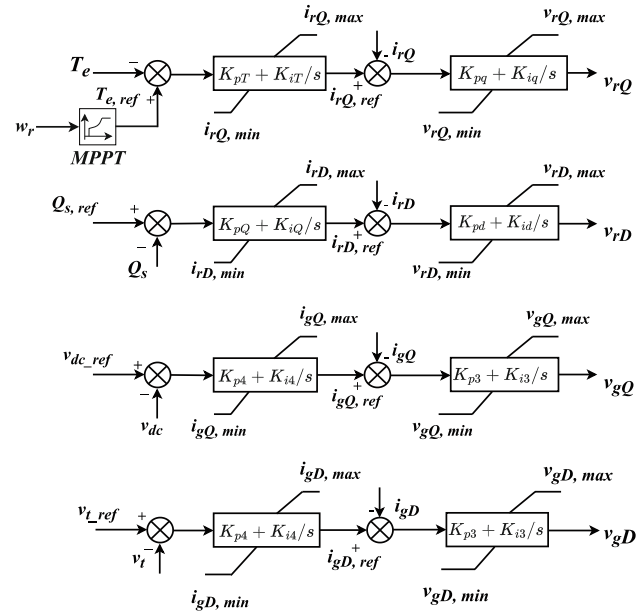


Fig. 5 Control structure of DFIG

3.6 Controller dynamic equations

Cascade structure-based controller shown in Fig. 5 is used in this work. Fast inner loop controls the currents. Slower outer loop of both RSC and GSC controls the parameters defined by the control objective. In this case, RSC controller is set to control electromagnetic torque and stator reactive power. The GSC controller has to control DC-link voltage and voltage at the DFIG terminals by supplying appropriate reactive power to grid via GSC. The equations corresponding to RSC and GSC controllers are listed as follows [24].

3.6.1 Dynamic model of RSC controller

Electric torque controller

$$\frac{di_{rQF}}{dt} = K_{iT}(T_{e, ref} - (-T_e)) = K_{iT}(k_{opt}\omega_r^2 + T_e) \tag{33a}$$

$$\frac{dv_{rQ1}}{dt} = K_{iQ}i_{rQF} + K_{iQ}K_{pT}(k_{opt}\omega_r^2 + T_e) - K_{iQ}i_{rQ} \tag{33b}$$

$$v_{rQ} = v_{rQ1} + K_{pQ}i_{rQF} + K_{pQ}K_{pT}k_{opt}\omega_r^2 + K_{pQ}K_{pT}T_e - K_{pQ}i_{rQ} \tag{33c}$$

Stator reactive power controller

$$\frac{di_{rDF}}{dt} = K_{iQ}(Q_{s, ref} - Q_s) \tag{34a}$$

Table 4 List of eigenvalues, damping factors (ζ) and dominant states (DS) for PQ and $V_w - Q$ case

Eigenvalues, damping factors and dominant states				$V_w - Q, V_w = 11.2, Q = 0.1, Q_{gsc} = 0.05$		
PQ, $P = 0.68, Q = 0.1, Q_{gsc} = 0.05$		Non-Iterative		Iterative		
Iterative		Non-Iterative		Eigenvalues	ζ	DS
Eigenvalues	ζ	Eigenvalues	ζ	Eigenvalues	ζ	DS
$-1.143 \times 10^6 \pm j299.3$	1	$-1.143 \times 10^6 \pm j299.4$	1	$-1.143 \times 10^6 \pm j307.44$	1	i_{lD}, i_{lQ}
$-10.3 \pm j313.43$	0.0328	$-10.3 \pm j313.43$	0.0328	$-10.3 \pm j313.43$	0.0328	ψ_{sD}, ψ_{sQ}
$-2.193 \pm j139.15$	0.0157	$-2.193 \pm j139.15$	0.0157	$-2.158 \pm j139.05$	0.0155	ω_r, T_{lg}
$-8.32 \pm j75.52$	0.109	$-8.32 \pm j75.52$	0.109	$-8.27 \pm j75.55$	0.109	i_{rQ1}, ψ_{rQ}
$-10.63 \pm j54.9$	0.190	$-10.63 \pm j54.9$	0.190	$-10.72 \pm j54.89$	0.191	ψ_{rD}, i_{rD1}
$-1.36 \pm j21.31$	0.064	$-1.36 \pm j21.31$	0.064	$-1.36 \pm j21.31$	0.0637	i_{gD}, v_{gD1}
$-1.294 \pm j20.86$	0.062	$-1.294 \pm j20.86$	0.062	$-1.294 \pm j20.86$	0.062	v_{gQ1}, i_{gQ}
-3.353	1	-3.352	1	-3.36	1	i_{rQF}, ω_{rt}
-1.785	1	-1.78	1	-1.78	1	i_{rDF}, v_{rD1}
-0.211	1	-0.211	1	-0.209	1	ω_{rt}, ω_r
$-0.0245 \pm j0.2200$	0.1107	$-0.0245 \pm j0.2200$	0.1106	$-0.0245 \pm j0.220$	0.1107	v_{dc}
-0.000203	1	-0.000203	1	-0.000204	1	i_{gDF}, i_{lD}

$$\begin{aligned} \frac{dv_{rD1}}{dt} &= K_{id}i_{rDF} + K_{id}K_{pQ}(Q_{s,ref} - Q_s) - K_{id}i_{rD} \\ v_{rD} &= v_{rD1} + K_{pd}i_{rDF} + K_{pd}K_{pQ}Q_{s,ref} \\ &\quad - K_{pd}K_{pQ}Q_s - K_{pd}i_{rD} \end{aligned} \tag{34b}$$

Reactive power flow from stator of DFIG to grid is given as

$$Q_s = v_s D i_{sQ} - v_s Q i_{sD} \tag{35}$$

3.6.2 Dynamic model of GSC controller

DC-link capacitor voltage controller

$$\frac{di_{gQF}}{dt} = K_{i4}(v_{dc,ref} - v_{dc}) \tag{36a}$$

$$\begin{aligned} \frac{dv_{gQ1}}{dt} &= K_{i3}i_{gQF} + K_{i3}K_{p4}(v_{dc,ref} - v_{dc}) - K_{i3}i_{gQ} \\ v_{gQ} &= v_{gQ1} + K_{p3}i_{gQF} + K_{p3}K_{p4}v_{dc,ref} \\ &\quad - K_{p3}K_{p4}v_{dc} - K_{p3}i_{gQ} \end{aligned} \tag{36b}$$

Terminal voltage controller

$$\frac{di_{gDF}}{dt} = K_{i4}(v_{t,ref} - v_t) \tag{37a}$$

$$\begin{aligned} \frac{dv_{gD1}}{dt} &= K_{i3}i_{gDF} + K_{i3}K_{p4}(v_{t,ref} - v_t) - K_{i3}i_{gD} \\ v_{gD} &= v_{gD1} + K_{p3}i_{gDF} + K_{p3}K_{p4}v_{t,ref} \\ &\quad - K_{p3}K_{p4}v_t - K_{p3}i_{gD} \end{aligned} \tag{37b}$$

3.7 Modelling of DC-link capacitor voltage controller

The DC-link capacitor which is a source of reactive power helps in supplying magnetizing currents to the DFIG [1]. The corresponding dynamic equation of DC-link capacitor is

$$\frac{dv_{dc}}{dt} = \frac{1}{Cv_{dc}}(P_r - P_{gsc}) \tag{38}$$

where C, v_{dc} are DC-link capacitance and its voltage, respectively, and their values are given in appendix. The active power flow from GSC to grid is given as

$$P_{gsc} = v_g D i_{gD} + v_g Q i_{gQ} \tag{39}$$

4 Case studies

The initial values calculated from iterative and non-iterative methods are tested on a 2 MW DFIG interfaced to an infinite bus (see Fig. 8). The initial values calculated are utilized to carry out eigenvalue analysis by linearizing dynamic equations around these steady-state values. Steady-state values

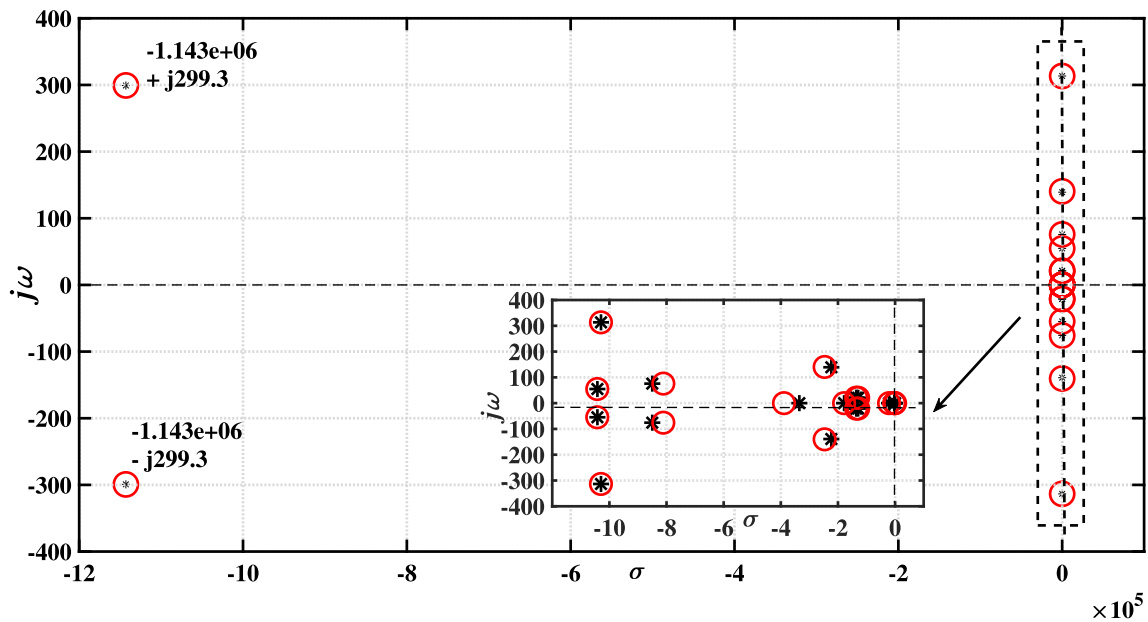


Fig. 6 Eigenvalues comparison for iterative and non-iterative case

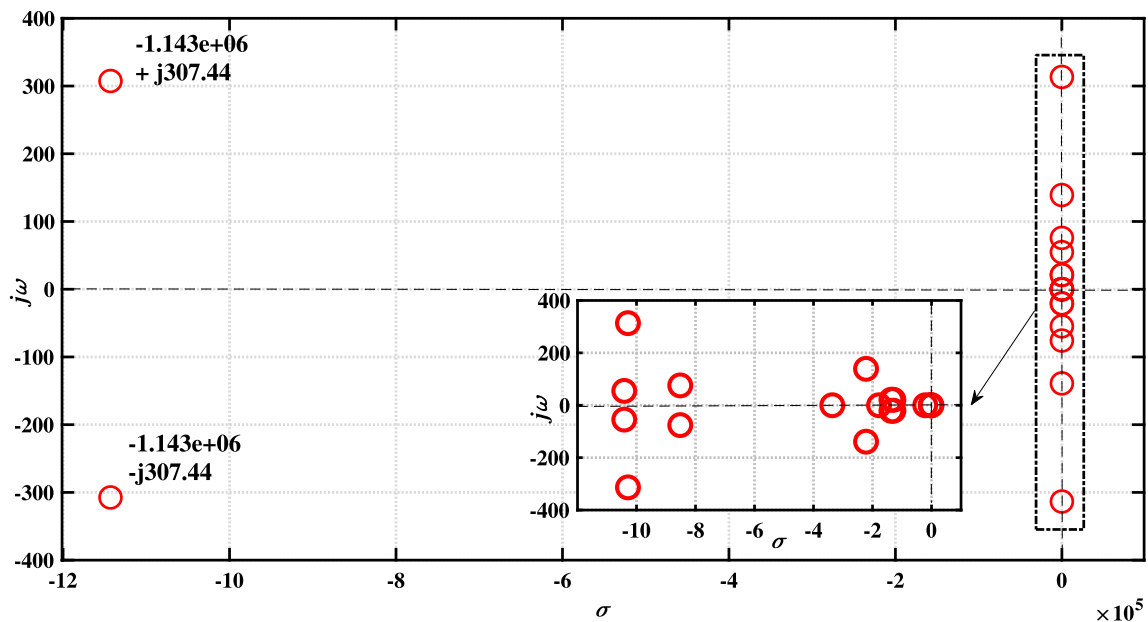


Fig. 7 Eigenvalue plot for $V_w - Q$ case

also act as initial values for integrator blocks in time-domain simulation model. Filter resistance and reactance values are given in appendix. For parameters of other subsystems of a DFIG-based WTS refer [25]. For gains of GSC controller refer [26]. For eigenvalues the dynamic equations are linearized around a steady-state value obtained from Sect. II. Time-domain simulations are conducted to complement results of eigenvalue analysis. Modal analysis and time-domain simulations are performed in MATLAB/Simulink software.

4.1 Eigenvalue analysis

Table 4 compares the eigenvalues obtained for PQ case with both iterative and non-iterative methods. It is seen that all the eigenvalues are on the left-half of the s-plane, which indicates the system is stable. Eigenvalues corresponding to iterative case are indicated with circle. Eigenvalues corresponding to non-iterative case are indicated with cross. As two of the eigenvalues are very large in magnitude, remaining eigenvalues are close to imaginary axis. In order to observe these

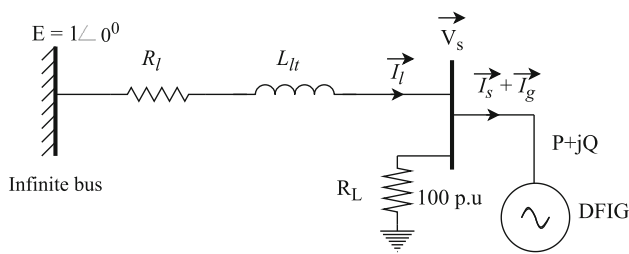


Fig. 8 DFIG interfaced to infinite bus

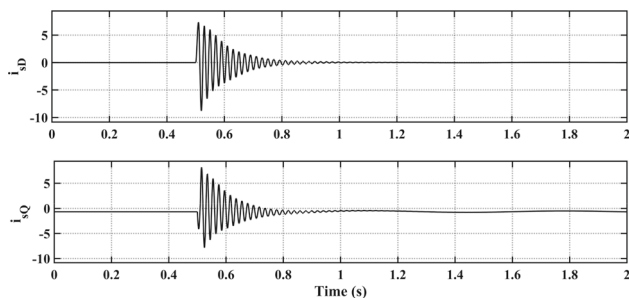


Fig. 9 Simulation plots of currents for PQ case with iterative method

eigenvalues a zoomed-in plot of eigenvalues which are close to imaginary axis is plotted within the main plot.

Figure 7 shows the eigenvalues for $V_w - Q$ case. It is seen that all the eigenvalues are on the left-half of s-plane, which indicates the considered system is stable. Also indicating that the steady-state values calculated are accurate as it maintains the system stable. For analysis with $V_w - Q$ method, the operating point is deliberately chosen as $V_w = 11m/s$, $Q = 0.1$, $Q_{gsc} = 0.05$., from the chosen wind speed, P calculated is 0.6801, which is almost equal to the P defined in PQ method. However, final initial values obtained from $V_w - Q$ method slightly differ to that of PQ method. This difference in initial values would reflect as variation in final eigenvalues as observed from Table 4. However, to complement the eigenvalue results, time-domain simulation plots are needed to accurately judge the effectiveness of the initialization approach used. The time-domain plots should have a flat start without any initial oscillations and should not destabilize the system when a small disturbance is introduced. From Figs. 6 and 7, it is concluded that the steady-state values computed are accurate as eigenvalue plot shows that the system is stable. Table 4 lists all the eigenvalues for PQ and $V_w - Q$ cases, for PQ procedure eigenvalues are listed for both iterative and non-iterative methods. Apart from eigenvalues, damping factors and dominant states in each mode are also listed. Participation factor analysis is performed to identify the dominant states in each mode. It is to be noted that dominant states in each mode are same in all the cases considered.

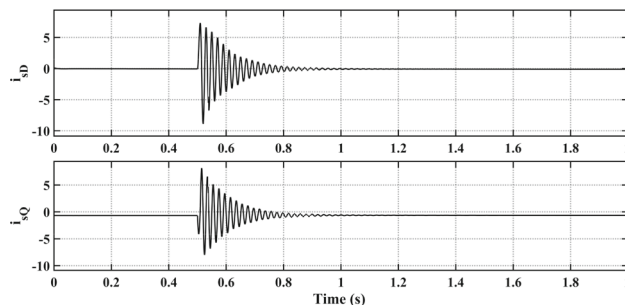


Fig. 10 Simulation plots of currents for PQ case with non-iterative method

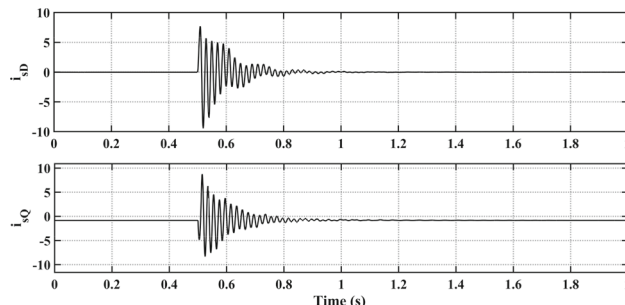


Fig. 11 Simulations plot of currents for $V_w - Q$ case

4.2 Time-domain simulations

The time-domain simulations are shown in Fig. 9 to Fig. 13. Figure 9 shows time-domain simulation plots for the case PQ using iterative method. Plots of i_{sD} , i_{sQ} that is stator currents are shown, with a small disturbance introduced at 0.5 s of simulation time. The currents plots shown are starting as a straight line without any oscillations and settling to steady-state value after a disturbance is cleared at 0.01 s of the fault occurrence.

Figure 10 shows plots of currents i_{sD} , i_{sQ} with case PQ for non-iterative method (using initial conditions obtained from non-iterative method). A small disturbance is introduced at 0.5 s by perturbing voltage at infinite bus for 0.01 s. From the simulations plots, it is observed that currents are settling to a steady-state value after the disturbance and also has a flat start initially, equal to the value calculated from non-iterative initialization method.

In Fig. 11, time-domain simulation plots are shown for case $V_w - Q$. Same disturbance is considered as of above two cases. Similar to the above plots there are no initial oscillations and the current values are starting at the initial values obtained from the steady-state calculation procedure. Also, the currents are settling to the steady-state after the disturbance, which indicates the initial values calculated are accurate and the system is dynamically stable.

Figures 12 and 13 compare the rotor speed and electromagnetic trajectories for the various initialization methods

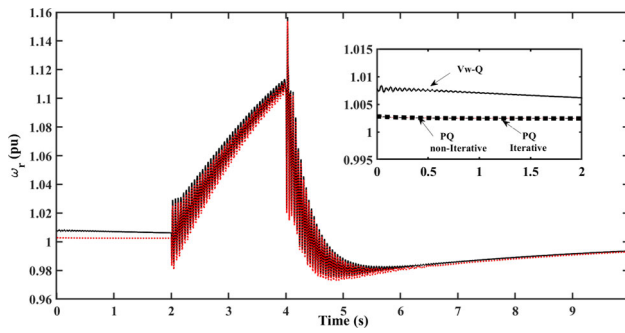


Fig. 12 Comparison of rotor speed trajectories for different initialization methods

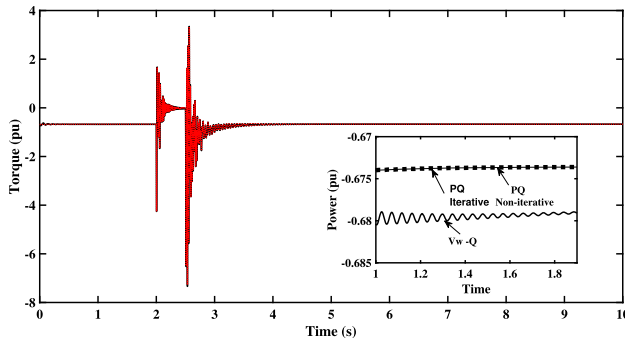


Fig. 13 Comparison of electromagnetic torque trajectories for different initialization methods

considered. A fault of duration 0.5 s is initiated at 2 s to observe behaviour of rotor speed and electromagnetic torque following a fault for different initialization methods. It is seen from the plots that both rotor speed and electromagnetic torque in PQ method have flat start trajectories following same path in both iterative and non-iterative cases. However, trajectory obtained using V_w -Q method has slight variation in the initial values with small oscillations. To observe the difference a zoomed-in plot is shown within the main plot for both rotor speed and electromagnetic torque within the main plots. The variation for initial values in V_w can be attributed to variation in the initial values calculated from different initialization methods.

5 Conclusion

Two different methods to initialize the DFIG-based WTS are employed in this paper. The first method that is, PQ approach is solved by both iterative and non-iterative methods and steady-state results are compared. The second approach, i.e. $V_w - Q$ approach is solved by iterative approach. Eigenvalue analysis is performed on a full-order DFIG model to see the dynamic performance of the considered system. Time-domain simulations are performed by introducing a small

disturbance to see accuracy of the steady-state values computed. From eigenvalue results, it is seen that all the poles are on left half of the s-plane which indicates the system is stable. From simulation results, it is observed that the currents are having a flat start and are settling to the stable values without destabilization after the fault, which shows the system is stable.

The approaches discussed in this paper help in accurate initialization of the DFIG-based WTS. The approaches employed in this work are flexible to consider non-zero reactive power flow from rotor to grid and filter losses. Apart from DFIG initialization, steady-state initialization of other subsystems of WTS is also discussed in this paper. Validation of steady-state values is performed on a grid-connected DFIG-based WTS by eigenvalue analysis and time-domain simulations. GSC controller states and DC-link voltage controller states are also considered in the analysis.

Author Contributions DRK was involved in conceptualization, methodology, software, formal analysis, investigation, writing — original draft. NSM and SMK contributed to supervision, writing—review & editing, resources.

Funding Not applicable.

Data availability Not applicable.

Declarations

Conflict of interest The authors declare no competing interests.

Ethical approval Not applicable.

Appendices

Appendix A

In this appendix following parameters of WTS are listed as given in Ref. [10]

$$C_p = c_1 \left(\frac{c_2}{\lambda_i} - c_3 \beta - c_4 \right) e^{-\frac{c_5}{\lambda_i}}, \frac{1}{\lambda_i} = \frac{1}{\lambda + 0.08\beta} - \frac{0.035}{\beta^3 + 1}$$

where λ is tip-speed ratio given by $\lambda = \frac{\omega_{rim} R}{V_w}$, β = pitch angle. $c_1=0.22$, $c_2=116$, $c_3=0.4$, $c_4=5$, $c_5=21$.

The value of k_{opt} is calculated by, $k_{opt} = \frac{1}{2} \frac{\rho A C_p \omega_{opt}^3 R^3 \omega_{rim}^3}{s_B \lambda_{opt}^3} = 0.67031$ pu, where R = Rotor radius, $\omega_{rim} B$ = Nominal speed of turbine, s_B = Base MVA.

when, $\beta = 0^\circ$, we have $\lambda_{opt} = 8.1001$, and the corresponding $C_{p_{opt}} = 0.48$.

The considered parameters of GS filter are $L_g = 0.0225$ pu, $R_g = 0.012$ pu

parameters of DC link capacitors are $C = 0.014$ F, $v_{dc} = 1200$ V

Formula used for fixed point iteration method is $\vec{V}_s(k+1) = \vec{V}_1 + (\frac{P+jQ}{V_s(k)}) * Z_l$.

Transmission line resistance (R_l) is 0.002 pu. Transmission line reactance (X_l) (including transformer reactance (X_{tr})) is 0.02 pu

Appendix B

See Tables 5 and 6

Table 5 Parameters of the wind turbine

Parameter	Values
Density of air	1.225 kg/m ³
Rotor dia	75 m
Nominal speed of the rotor	18 rpm
Nominal speed of the wind	14 m/s
Cut-in speed of wind	5 m/s
Cut-out speed of wind	25 m/s

Table 6 Parameters for 2 MW DFIG

DFIG parameter	Values
Rated power of DFIG	2 MW
Rated voltage	690 V
Operating frequency	50 Hz
Rated p.f	0.9
Rated efficiency	0.9
Resistance of stator (R_s)	0.00488 pu
Resistance of rotor (R_r)	0.00549 pu
Leakage inductance of stator (X_s)	0.09241 pu
Leakage inductance of rotor (X_r)	0.09955 pu
Mutual inductance (X_m)	3.95279 pu
Generator rotor inertia constant (H_g)	0.5 s

References

1. Abad G, Lopez J, Rodríguez M, Marroyo L, Iwanski G (2011) Introduction to a wind energy generation system
2. Fan L, Miao Z (2015) Modeling and analysis of doubly fed induction generator wind energy systems. Academic Press, Cambridge
3. Gianto R (2021) Steady-state model of DFIG-based wind power plant for load flow analysis. IET Renew Power Gener 15(8):1724–1735
4. Amutha N, Kumar BK (2014) Initialization of DFIG based wind generating system. In: 2014 eighteenth national power systems conference (NPSC). IEEE, pp 1–5
5. Padrón JFM, Lorenzo AEF (2009) Calculating steady-state operating conditions for doubly-fed induction generator wind turbines. IEEE Trans. Power Syst. 25(2):922–928
6. Karthik DR, Kotian SM, Manjarekar NS (2021) Steady-state initialization of doubly fed induction generator based wind turbine considering grid side filter. In: 2021 13th IEEE PES Asia pacific power energy engineering conference (APPEEC). IEEE, pp 1–6
7. Kumar Seshadri Sravan V, Thukaram D (2018) Accurate modeling of doubly fed induction generator based wind farms in load flow analysis. Electr Power Syst Res 155:363–71
8. Ledesma P, Usaola J (2005) Doubly fed induction generator model for transient stability analysis. IEEE Trans Energy Convers 20(2):388–397
9. Karthik DR, Kotian SM, Manjarekar NS (2022) An accurate method for steady state initialization of doubly fed induction generator. In: 2022 IEEE international conference on power electronics, smart grid, and renewable energy (PESGRE). IEEE, pp 1–6
10. Sloopweg JG, Polinder H, Kling WL (2001) Initialization of wind turbine models in power system dynamics simulations. In: 2001 IEEE Porto power tech proceedings (Cat. No. 01EX502), Vol 4. IEEE, pp 6
11. Holdsworth L, Wu XG, Ekanayake JB, Jenkins N (2003) Direct solution method for initialising doubly-fed induction wind turbines in power system dynamic models. IEE Proc Gener Transm Distrib 150(3):334–342
12. Wu M, Xie L (2017) Calculating steady-state operating conditions for DFIG-based wind turbines. IEEE Trans Sustain Energy 9(1):293–301
13. Alejandro Joaquín P (2019) Initialization of DFIG wind turbines with a phasor-based approach. Wind Energy 22(3):420–32
14. Louie KW, Wang A, Wilson P, Buchanan P (2005) Discussion on the initialization of the EMTP-type programs. In: Canadian conference on electrical and computer engineering, pp 1962–1965. IEEE
15. Feijoo A, Villanueva D (2016) A PQ model for asynchronous machines based on rotor voltage calculation. IEEE Trans Energy Convers 31(2):813–814

16. Eminoglu U, Dursun B, Hocaoglu MH (2009) Incorporation of a new wind turbine generating system model into distribution systems load flow analysis. *Wind Energy Int J Progress Appl Wind Power Convers Technol* 12(4):375–390
17. Feijóo A (2009) On PQ models for asynchronous wind turbines. *IEEE Trans Power Syst* 24(4):1890–1891
18. Huang C (2018) Two RX models of doubly-fed induction generators for load flow analysis. In: 2018 2nd IEEE conference on energy internet and energy system integration (EI2). IEEE, pp 1–6
19. Muller S, Deicke M, De Doncker RW (2002) Doubly fed induction generator systems for wind turbines. *IEEE Ind Appl Mag* 8(3):26–33
20. de Wekken TV, Wein F Power quality and utilization guide section-8. In: KEMA consulting Distributed generation Leonard Energy Autumn
21. Manwell JF, McGowan JG, Rogers AL (2010) *Wind energy explained: theory, design and application*. Wiley, New York
22. Ekanayake JB, Holdsworth L, Wu X, Jenkins N (2003) Dynamic modeling of doubly fed induction generator wind turbines. *IEEE Trans Power Syst* 18(2):803–809
23. Padiyar KR (2006) *Power system dynamics—stability and control*. BS Publications, Hyderabad
24. Fan L, Kavasseri R, Miao ZL, Zhu C (2010) Modeling of DFIG-based wind farms for SSR analysis. *IEEE Trans Power Deliv* 25(4):2073–2082
25. Prasanthi E, Shubhanga KN (2016) Stability analysis of a grid connected DFIG based WECS with two-mass shaft modeling. In: 2016 IEEE annual India conference (INDICON). IEEE, pp 1–6
26. Fan L, Zhu C, Miao Z, Hu M (2011) Modal analysis of a DFIG-based wind farm interfaced with a series compensated network. *IEEE Trans Energy Convers* 26(4):1010–1020

Publisher's Note Springer Nature remains neutral with regard to jurisdictional claims in published maps and institutional affiliations.

Springer Nature or its licensor (e.g. a society or other partner) holds exclusive rights to this article under a publishing agreement with the author(s) or other rightsholder(s); author self-archiving of the accepted manuscript version of this article is solely governed by the terms of such publishing agreement and applicable law.